DispatchDate: 13.11.2019 · ProofNo: 385, p.1

nature chemistry

ARTICLES

https://doi.org/10.1038/s41557-019-0385-8

Achieving spin-triplet exciton transfer between silicon and molecular acceptors for photon upconversion

Pan Xia[1,5], Emily K. Raulerson[2,5], Devin Coleman[3], Carter S. Gerke[4], Lorenzo Mangolini[3]*, Ming Lee Tang[1,4]* and Sean T. Roberts[2]*

Inorganic semiconductor nanocrystals interfaced with spin-triplet exciton-accepting organic molecules have emerged as promising materials for converting incoherent long-wavelength light into the visible range. However, these materials to date have made exclusive use of nanocrystals containing toxic elements, precluding their use in biological or environmentally sensitive applications. Here, we address this challenge by chemically functionalizing non-toxic silicon nanocrystals with triplet-accepting anthracene ligands. Photoexciting these structures drives spin-triplet exciton transfer from silicon to anthracene through a single 15 ns Dexter energy transfer step with a nearly 50% yield. When paired with 9,10-diphenylanthracene emitters, these particles readily upconvert 488–640 nm photons to 425 nm violet light with efficiencies as high as 7 ± 0.9% and can be readily incorporated into aqueous micelles for biological use. Our demonstration of spin-triplet exciton transfer from silicon to molecular triplet acceptors can critically enable new technologies for solar energy conversion, quantum information and near-infrared driven photocatalysis.

Materials that convert infrared light into the visible range are desirable as they can enable advanced schemes for photocatalysts[1], solar energy harvesting[2], deep tissue imaging[3] and phototherapy[4]. Inorganic nanocrystals (NCs) functionalized with energy-accepting dyes form a promising platform to meet this demand. These materials achieve light upconversion by using photons absorbed by the NC to excite spin-triplet excitons centred on organic molecules tethered to their surface[5–7]. Pairs of these excitons can merge through a process known as triplet fusion to produce high-energy spin-singlet states that emit visible light. Although upconversion efficiencies of >10% have been achieved by this approach[8,9], these systems have exclusively employed NCs containing toxic heavy elements such as cadmium or lead (refs. [5,6,10]), limiting their range of utility. Replacement of these NCs with non-toxic infrared absorbers is a key step in designing upconversion systems suitable for both biological and environmental applications.

In this context, silicon is highly attractive for NC-based upconversion systems as it is earth-abundant and non-toxic. Methodologies exist for producing silicon nanocrystals (Si NCs) in large quantities[11,12] and synthetic approaches are available for attaching ligands to their surfaces through strong covalent silicon–carbon bonds[13]. Moreover, tethering spin-triplet exciton-accepting dyes to Si NCs is attractive not only for photon upconversion, but also for functional interfaces that extract spin-triplet excitons produced by singlet fission, the inverse of triplet fusion. Singlet fission is highly efficient in a number of polycyclic aromatic hydrocarbon solids and molecular dimers[14–22], and pairing this process with inorganic semiconductors offers potential for photovoltaics that surpass the Shockley–Queisser limit[2,23,24] and quantum information devices that employ spin-entangled exciton pairs[25]. Due to its dominance within the semiconductor industry, silicon represents a natural material partner and recent work reported by Baldo and co-workers on tetracene:silicon junctions has shown spin-triplet exciton transfer from tetracene to silicon (ref. [26]). Although promising, Baldo was unable to identify a triplet exciton transfer mechanism and noted that the interfacial structure of the tetracene:silicon junction had to be carefully controlled to observe any energy transfer. In this respect, dye-functionalized Si NCs could greatly aid the optimization of organic:silicon junctions by allowing triplet energy transfer to be studied in the absence of complicating effects such as exciton diffusion to and from the interface.

Here, we demonstrate that Si NCs produced by a non-thermal plasma synthesis can be readily functionalized with anthracene triplet acceptors to produce photon upconversion systems that convert 488–640 nm photons into 425 nm violet light with efficiencies as high as 7 ± 0.9% and saturation threshold intensities as low as 950 mW cm^{-2}. These materials can be readily incorporated into aqueous micelles for biological imaging and upconvert light to a limited degree even in the presence of oxygen. Using femtosecond transient absorption (TA) spectroscopy, we find silicon-to-anthracene triplet energy transfer occurs through the concerted transfer of an electron and hole (Dexter energy transfer) over 15 ns, a rate comparable to that achieved with direct bandgap NC systems[7,27,28], which we achieve through the use of the short, covalent tether anchoring these materials. We also identify energetic matching between the triplet exciton energies of the anthracene acceptors and Si NCs to be critical for achieving efficient energy transfer between them. Our work clearly demonstrates that spin-triplet exciton transfer between silicon and organic molecules is indeed possible, which is a critical step for the realization of biocompatible photon

[1]Materials Science & Engineering Program, University of California Riverside, Riverside, CA, USA. [2]Department of Chemistry, The University of Texas at Austin, Austin, TX, USA. [3]Department of Mechanical Engineering, University of California Riverside, Riverside, CA, USA. [4]Department of Chemistry, University of California Riverside, Riverside, CA, USA. [5]These authors contributed equally: Pan Xia, Emily K. Raulerson. *e-mail: lmangolini@engr.ucr.edu; mltang@ucr.edu; roberts@cm.utexas.edu

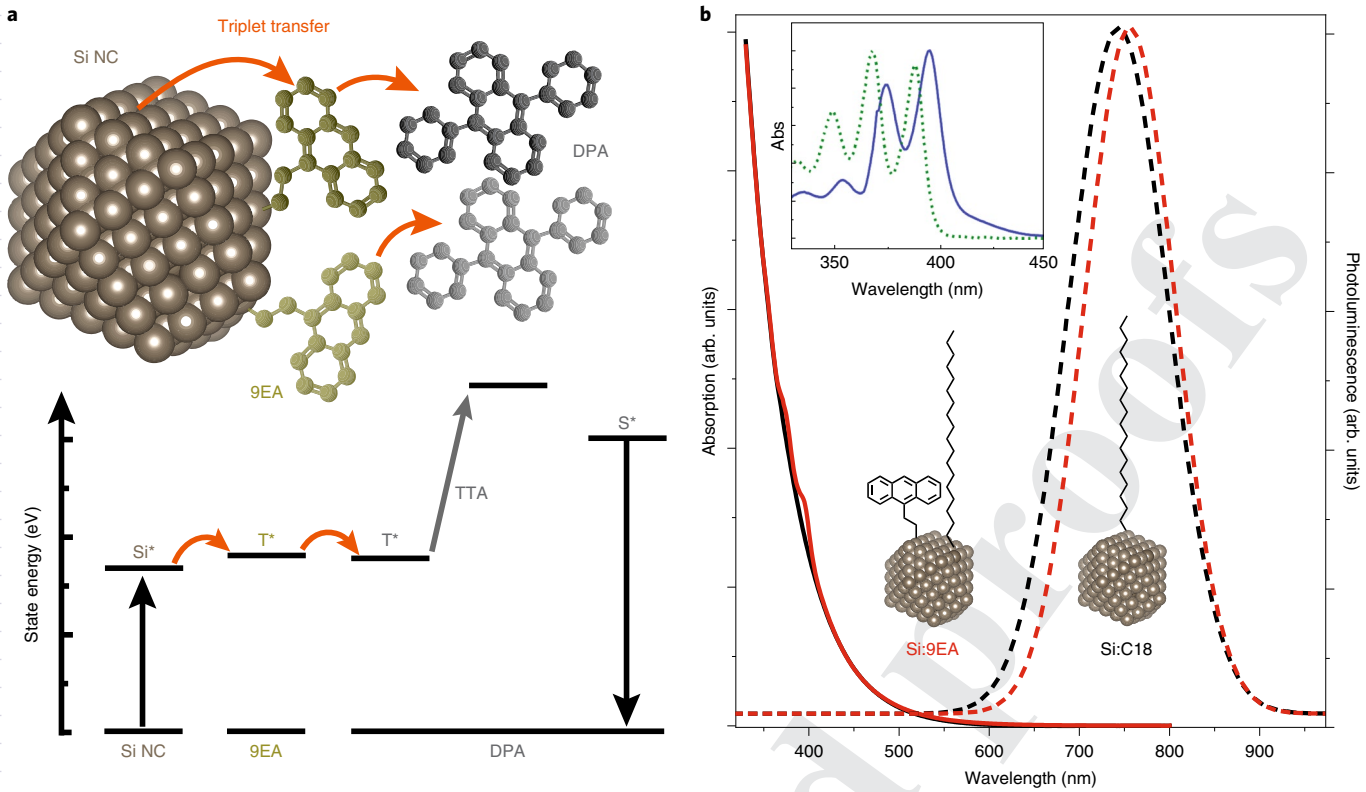

Fig. 1 | State energies and spectra of the upconverting system. a, Schematic illustration of photon upconversion based on Si NCs. Light absorbed by Si NCs produces an excited electron–hole pair that transfers to 9EA, forming a molecular spin-triplet exciton. Excited 9EA molecules then transfer these excitons to DPA molecules diffusing in solution. Higher-energy photons are emitted after TTA occurs between pairs of excited DPA molecules. **b**, Absorption spectra (solid lines) and emission spectra (dashed lines, $\lambda_{Ex} = 488$ nm) of Si NCs functionalized with only octadecane (Si:C18, black) and a combination of octadecane and 9VA (Si:9EA, red) in toluene under argon at room temperature. Inset: 9EA bound to Si exhibits a noticeable redshift in its absorption features (blue solid line) in comparison with 9MA (blue dashed line), which is indicative of electronic interactions between Si and 9EA. Note, anthracene features seen in Si:9EA samples belong only to surface-bound anthracene as any free 9VA in solution has been removed by repeated washing.

upconversion systems, singlet-fission-based solar cells and quantum information devices.

Results

Figure 1a illustrates the nanocrystal-to-molecule triplet energy transfer scheme we employed for photon upconversion. In this scheme, low-energy photons absorbed by a Si NC produce electron–hole pairs (excitons) that pass their energy to 9,10-diphenylanthracene (DPA) molecules in solution, exciting them to a spin-triplet exciton state. When two excited DPA molecules encounter one another, they can undergo triplet–triplet annihilation (TTA), in which one is de-excited while the other is promoted to a high-energy emissive spin-singlet state that proceeds to fluoresce. Previous work by our group[6,29,30] and others[7,10,31,32] showed that attachment of molecular triplet-accepting molecules to ionic chalcogenide NC triplet photosensitizers can significantly enhance photon upconversion by acting as a transmitter layer that facilitates energy transfer to molecules in solution. However, as Si NCs bind ligands through strong covalent bonds[13], the attachment of triplet transmitting molecules to these NCs requires chemistries that allow the covalent attachment of acceptors while limiting the propensity of the NCs to oxidize when exposed to trace amounts of water and oxygen. To this end, we chose to work with highly crystalline Si NCs synthesized by the non-thermal plasma reduction of silane with hydrogen in the presence of argon (ref. [11]). Compared with silicon nanoparticles made by other methods, the resulting surface hydride (SiH_x) makes these NCs amenable to thermal hydrosilylation. As detailed in the Supplementary Information, the Si NCs were thermally hydrosilylated with either 1-octadecene or a combination of 1-octadecene and 9-vinylanthracene (9VA), which converts into 9-ethylanthracene (9EA) on attachment. This yields two functionalized Si NC samples, one with a ligand shell containing only octadecane, which we label Si:C18, and a second containing a mixed ligand shell of octadecane and 9EA, which we denote Si:9EA for brevity (Fig. 1b).

Unlike direct gap semiconductor NCs, Si NCs have a relatively featureless absorption spectrum, reflecting their indirect bandgap (Fig. 1b, black). In line with previous reports, Si:C18 exhibits broad steady-state photoluminescence with an emission quantum yield (QY) of 16.1 ± 2.2% that peaks at 741 nm, indicating a particle diameter of 3.1 nm based on known sizing curves[33]. Upon hydrosilylation with 9VA, the NC emission is redshifted by 46 meV and decreases in quantum efficiency to 8.2 ± 1.2% (Fig. 1b). In parallel, distinct features appear in the absorption spectrum of Si:9EA that are indicative of surface-bound anthracene, but are notably redshifted by 55 meV relative to those of free 9-methylanthracene (9MA) in toluene (Fig. 1b, inset). This shift is larger than that seen for comparable acene molecules bound to ionic chalcogenide NCs[9,34–36], suggesting stronger electronic interaction between 9EA and the Si NC core. From the electronic absorption spectrum of Si:9EA, we estimate the average number of 9EA molecules bound to each Si NC, N_{9EA}, to be 2 (Supplementary Information, Section 2). Nuclear magnetic resonance (Supplementary Fig. 3) and attenuated total reflectance infrared spectroscopy (Supplementary Fig. 4) also confirmed the presence of surface-bound 9VA. We note that the infrared spectra signal some oxidation of the functionalized Si NCs

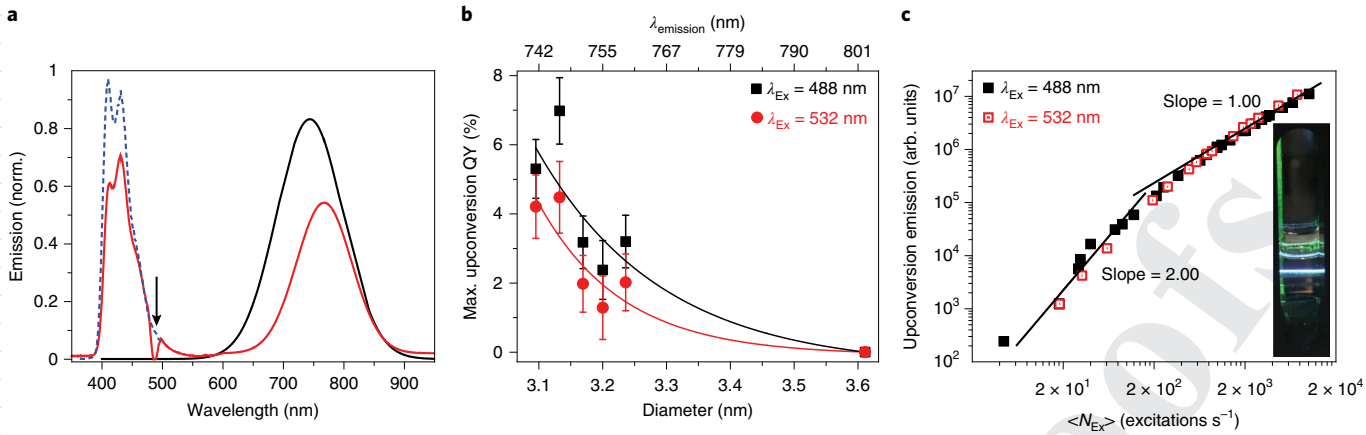

Fig. 2 | Quantification of the upconverted photoluminescence spectra. a, Photoluminescence spectra of 3.1 nm diameter Si NCs bearing only octadecane (Si:C18, black), Si NCs bearing octadecane and 9EA functionalization (Si:9EA, red) and only DPA (blue, λ_{Ex} = 350 nm). Inset: excitation with green 532 nm light creates visible upconverted blue emission from DPA. **b**, Dependence of the photon upconversion QY on Si NC diameter showing that as the NC size decreases, the upconversion QY increases. Solid lines are drawn as a guide to the eye. Error bars denote a standard deviation of one. **c**, A log–log plot of the upconverted emission intensity of Si:9EA|DPA vs. N_{Ex}, the average number of times a NC is photoexcited per second under continuous-wave illumination. The upconversion emission intensity shows a transition from quadratic (slope = 2) to linear (slope = 1) regimes. Inset: upconverted emission in a cuvette after 488 nm excitation.

even when stored in a nitrogen glovebox with water < 0.5 ppm and oxygen < 0.2 ppm. This has been observed in Si NCs prepared by thermal hydrosilylation[37] and does not appear to be a severe barrier to triplet energy transfer.

Photon upconversion measurements were performed under nitrogen with Si NC light absorbers and DPA molecular emitters in toluene at room temperature. In this multi-step triplet-based process, DPA emits violet light after combining the energy originating from two photons of lower energy. DPA was chosen because of its high (>97%) fluorescence QY and long-lived, low-lying first-excited triplet state (E = 1.77 eV, ref. [38]), which provides a small energetic driving force for triplet energy transfer from surface-bound 9EA (E = 1.8 eV, refs. [38,39]). We find no evidence of photon upconversion with Si:C18 as triplet photosensitizer in 5.2 mM DPA (Fig. 2a). This was expected as the octadecane ligand shell presents a formidable barrier to triplet energy transfer, which depends exponentially on the spatial separation of the energy donor and acceptor[40]. In contrast, Si:9EA displays ready photon upconversion when illuminated with visible light in the presence of DPA, achieving upconversion QYs as high as 7.0 ± 0.9% when small 3.1–3.2 nm diameter Si NCs are employed (Fig. 2b and Supplementary Fig. 2). Here, we have defined the upconversion QY to have a maximum value of 100%, meaning that 7% of absorbed photons go on to produce upconverted photons.

An important parameter for upconversion systems is the excitation rate threshold, the point at which the upconverted light intensity switches from a quadratic to a linear dependence on incident power. Above this threshold, TTA ceases to be rate-limiting as the steady-state triplet population in the system is sufficiently high that any photoexcited molecule will find an excited partner within their lifetime to undergo TTA. We find that for Si:9EA, this threshold falls at 0.95 W cm^{-2} for a 488 nm exciting source (Fig. 2c) and doubles to 2 W cm^{-2} for 532 nm light, reflecting the decreased absorption by the Si NCs at 532 nm compared with at 488 nm. This was confirmed by plotting the upconversion intensity as a function of the excitation rate of the NCs, which shows that the data obtained with the 488 and 532 nm excitation sources are overlaid (Fig. 2c). Under 640 nm excitation, a relatively low photon upconversion QY of 0.10 ± 0.07% was measured (Supplementary Fig. 2), showing that low-energy photons can drive upconversion despite the low optical density of Si NCs at this long wavelength.

Importantly, we find that the upconverted photon quantum efficiency depends on Si NC size (Fig. 2b), increasing from about 0 to 7% as the NC diameter decreases from 3.6 to 3.1 nm. Efforts to examine this trend further by producing smaller Si NCs yielded particles that were not colloidally stable after octadecane functionalization. The bandgap of Si NCs with aliphatic carbon ligands decreases with increasing Si NC diameter due to quantum confinement of charge carriers[37,41], as noted by the peak emission wavelengths of differently sized particles (Fig. 2b). This change in bandgap with NC size provides a clear hypothesis for the decrease in the upconversion QY that we observe, as reducing the silicon bandgap below the 9EA triplet energy (1.8 eV) will introduce a barrier for nanocrystal-to-molecule energy transfer.

To evaluate this hypothesis, we examined Si:C18 and Si:9EA using TA spectroscopy. Figure 3a (left) shows the spectral dynamics of Si:C18 after photoexcitation at 532 nm, which exhibit a set of broad induced absorption bands that relax over a series of time periods spanning a few nanoseconds to tens of microseconds. Such non-exponential decay has been noted previously for Si NCs (ref. [42]) and can be well reproduced by a fit model that assumes a Poisson distribution of quenching sites spread throughout the NC ensemble (Supplementary Information, Section 7).

Following 9EA functionalization, the TA spectra show the growth of a new induced absorption band peak at 435 nm and a photobleach at 395 nm that develop over a 22 ns timescale superimposed on the Si NC signal (Fig. 3a, right). Isolating this new feature by subtracting the silicon background yields the spectrum shown in Fig. 3b, which we assign to the 9EA triplet state, based on a comparison with triplet sensitization experiments (Supplementary Information, Section 5). Figure 3c shows the variation of both the 9EA triplet and the excited Si NC population with time, demonstrating that the rise of the triplet signal and decay of the Si NCs occur on the same timescale, indicating that 9EA triplet formation directly results from energy transfer from the Si NCs. These first-order kinetics are in strong contrast to the dynamics shown by other triplet-sensitizing NCs, such as PbS:pentacene, in which the NC surface states play a key role in transfer[35,43]. Rather, we see the direct production of 9EA triplets as Si NCs decay, implying that the transfer occurs in a single Dexter energy transfer step from the lowest-energy exciton band of silicon.

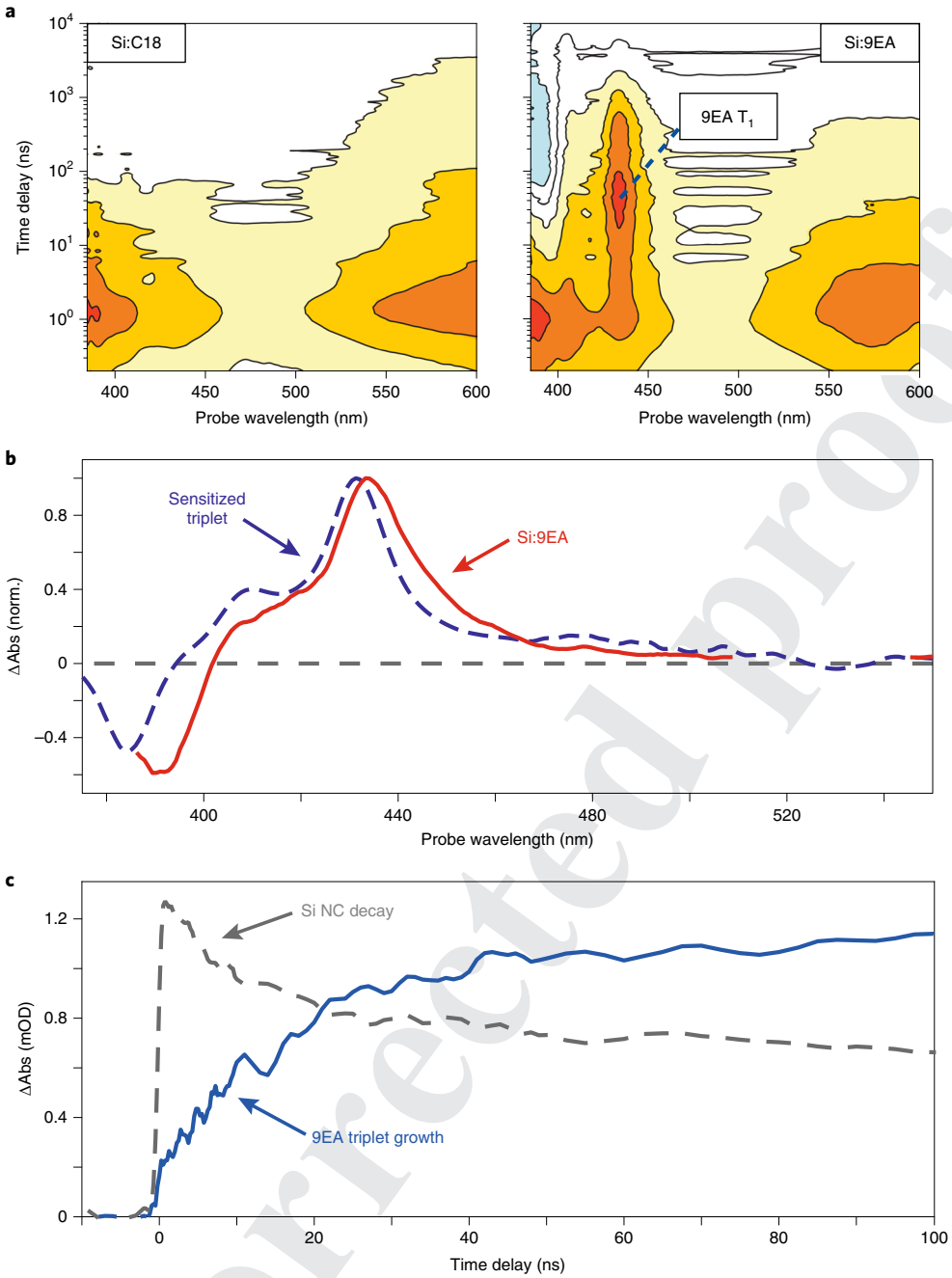

Fig. 3 | Kinetics of triplet energy transfer from Si NCs to 9EA. a, TA spectra of Si:C18 and Si:9EA excited at 532 nm. Left: TA contour plot showing the decay of the Si-NC-photoinduced absorption of Si:C18 following Si excitation. Right: TA contour plot of Si:9EA showing the growth of 9EA features, notably a photobleach at 395 nm (light-blue contour) and the induced absorption peak at 435 nm (red/orange contours), superimposed on the Si-induced absorption background. **b**, Comparison of the 9EA spectral features extracted from the Si:9EA TA data with those identified in 9EA triplet sensitization experiments confirming that 9EA triplets form following photoexcitation of Si in Si:9EA structures. **c**, Kinetic traces showing that 9EA triplet growth occurs on the same timescale as Si NC signal decay, with a persistent Si NC signal.

Discussion

Although it is tempting to assign the rate of 9EA signal growth to the Si-to-9EA Dexter energy transfer rate, this does not account for the fact that our Si:9EA ensemble consists of a distribution of variable-size NCs that bind differing numbers of 9EA molecules. The impact of this distribution is highlighted by the decay of the silicon signal (Fig. 3c), which persists after the 9EA triplet decays. This implies that not all photoexcited Si NCs transfer an exciton to 9EA, which can be explained if a subset of NCs bind no 9EA molecules. Assuming 9EA is distributed among the Si NCs according to a Poisson distribution, our prior estimate of 2 for N_{9EA} implies 13.5% of the NCs in our ensemble do not bind any 9EA molecules. Although this explains a portion of the persistent silicon signal at long time delays, it does not account for the shift of the NC emission energy that we observe upon 9EA functionalization. Rather, the triplet energy of 9EA (1.8 eV) is expected to introduce an energy barrier for triplet energy transfer for some of the NCs in our ensemble with narrower bandgaps. Any attempt to quantify the rate and

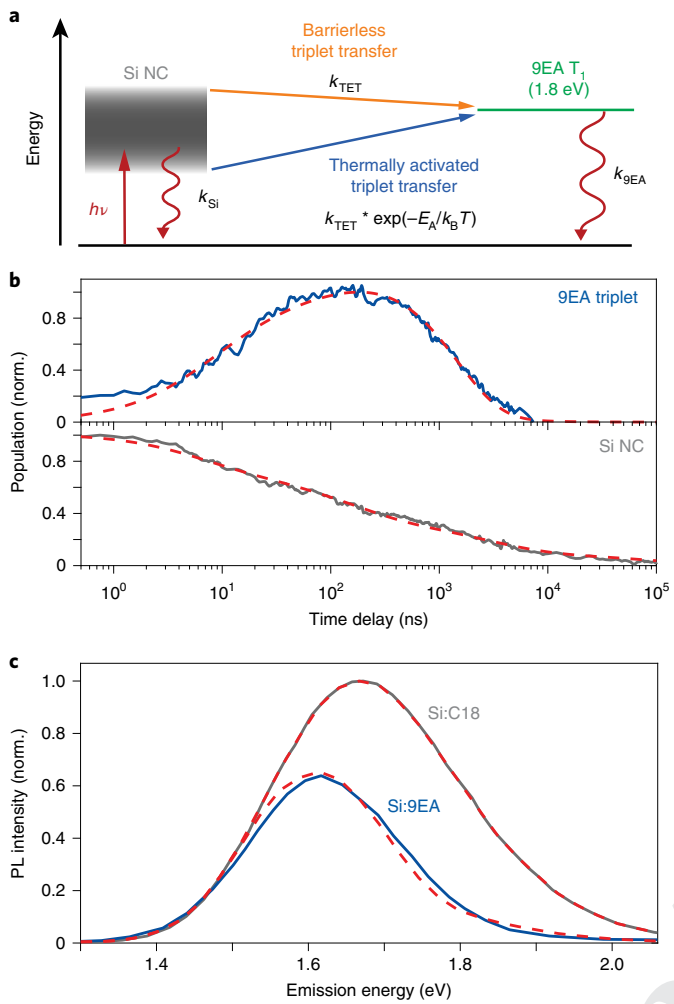

Fig. 4 | Using a kinetic model to fit time-resolved spectra. a, Kinetic model of triplet energy transfer and decay, including the energy barrier to triplet transfer due to the heterogeneity of the bandgaps of Si NCs. **b**, Fits to time-dependent populations of 9EA triplet excitons and excited Si NCs that faithfully reproduce the kinetics over five decades in time. We note that there is some discrepancy between the triplet population and the fit at short time delays, which is an artefact of the background normalization used to extract this population. **c**, The model in panel **a** reproduces the energy-dependent quenching of Si NC populations after functionalization with 9EA. PL, photoluminescence.

yield of triplet energy transfer from silicon to 9EA must account for these two effects.

A kinetic model that explains our transient results by accounting for two sources of heterogeneity that impact triplet energy transfer from silicon to 9EA is outlined in Fig. 4a. This model assumes our NC ensemble comprises a distribution of NCs with exciton energies described by the ensemble Si NC emission linewidth. Energy transfer from NCs with an exciton energy lower than the triplet energy of 9EA are taken to experience an Arrhenius activation barrier. Members of this ensemble are further taken to bind different numbers of 9EA molecules in accordance with a Poisson distribution with $N_{9EA}=2$. Solutions to kinetic equations given by this model and a description of our fitting procedure are given in Supplementary Information, Section 7. Decay parameters governing the intrinsic relaxation of Si:C18 NCs are assumed to be unchanged by 9EA functionalization, which leaves only two key free parameters to fit the growth and decay of the 9EA triplet population, the forward transfer rate constant, k_{TET}, and the 9EA decay rate constant, k_{9EA}. Figure 4b shows the result of this fitting process overlaid on the triplet and Si NC populations extracted from the Si:9EA TA data. Overall, we find very good agreement with our data over five decades of time, despite the model's limited number of free parameters. This model also reproduces the energy-dependent quenching of Si NC emission upon 9EA functionalization (Fig. 4c), first highlighted in Fig. 1b.

With these fits in hand, we can examine the overall yield for triplet energy transfer from Si NCs to 9EA. We find the intrinsic timescale of forward transfer is quite rapid, 15 ns, which implies that the slower rise of the 9EA triplet population in Fig. 4b in part arises from the thermal activation of the transfer. For these samples, we find that 48% of the excited NCs successfully transfer energy to 9EA. Of the remaining non-transferred excitations, we estimate that they result from NCs with no 9EA attached, larger NCs with exciton energies too low to effectively transfer to the 9EA triplet state and intrinsic decay pathways within the Si NCs. Importantly, improvements in synthetic methods that either stabilize smaller Si NCs, increase 9EA loading or replace 9EA with acceptors with lower triplet exciton energies can be straightforwardly used to address the first two of these three loss pathways, which, if eliminated, could be used to achieve transfer yields as high as 91% according to our model. Assuming a proportional gain in upconversion efficiency, this would suggest we can nearly double this value.

Although our data demonstrate that Si NCs can efficiently fuel triplet-fusion-based photon upconversion, biological applications require Si NCs to function in aqueous, oxygen-containing environments. Using methods adapted from the work of Sanders et al.[44], we have prepared micelles based on Poloxamer 188 (P188), a triblock copolymer comprising a hydrophobic core [poly(propylene oxide)] flanked by two hydrophilic poly(ethylene glycol) chains. P188 is a surfactant approved by the US Food and Drug Administration that is currently used in many over-the-counter products, including toothpaste, cosmetics and pharmaceuticals. Within the core of these micelles, Si:9EA NCs are dispersed in a small volume of *o*-dichlorobenzene (ODCB) along with DPA triplet-fusion photon upconverters (Fig. 5a). Dynamic light scattering experiments indicate that these micelles display an average diameter of 220 nm with a polydispersity index of 0.140 (Supplementary Fig. 6). This size is sufficiently small that these micelles are suitable for a range of biological applications.

Upon illumination under an inert argon atmosphere at either 488 or 512 nm, we observe upconverted emission from the DPA molecules (Fig. 5b), confirming that the Si NCs within the micelles are capable of transferring triplet excitons to surface-bound 9EA molecules followed by transfer to DPA. We find the upconverted emission varies linearly with the input excitation power, indicating that the diffusion of molecules within the micelles does not limit upconversion (Fig. 5c). Importantly, we find the micelles show exceptional stability when they are stored under an inert atmosphere. Fig. 5b displays the emission spectra of upconverting micelles recorded 4 and 17 hours after preparation. These two spectra are nearly identical, highlighting their stability under anaerobic conditions.

Remarkably, when these micelles are exposed to oxygen, a notorious triplet quencher, we find photon upconversion continues for 25 minutes (Fig. 5d). In this time frame, we find the Si NC band edge emission drops in intensity by half and undergoes a blueshift, which is expected for NCs undergoing surface oxidation, suggesting the decay of upconversion under aerobic conditions partially stems from the oxidation of silicon in addition to direct triplet quenching by oxygen. However, we note that in forming our micelles we have taken no explicit steps to block oxygen from reaching micelle interiors other than initially preparing them under argon. The replacement of P188 by other surfactants containing larger regions of saturated carbons that can pack more densely[45,46] and the

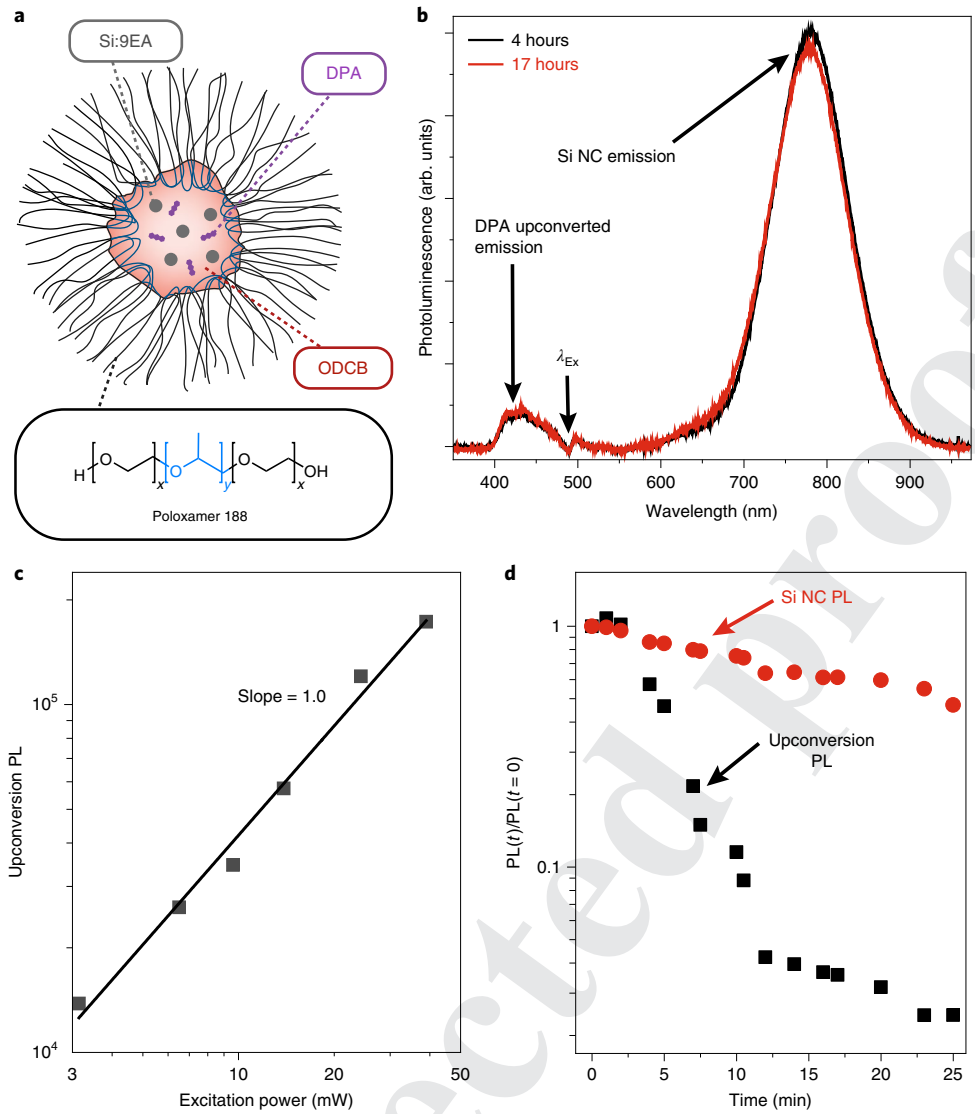

Fig. 5 | Si NC upconversion in an aqueous environment. a, Schematic of the aqueous photon upconverting micelles. **b**, Stability of photon upconversion in aqueous micelles under argon (λ_{Ex} = 488 nm). Particles are stable over multiple days with no observed degradation of upconversion emission. **c**, The upconversion emission in micelles shows a linear dependence on excitation power. **d**, As air exposure time increases, the upconversion photoluminescence decreases due to oxygen quenching of triplet states. Si NC photoluminescence also decreases, suggesting some oxidation of the NC surfaces. PL, photoluminescence.

addition of oxygen scavengers to micelle interiors[47] can each be used to improve the longevity of photon upconversion in aerobic, aqueous environments, increasing the potential of this system for biological applications.

In conclusion, we have demonstrated for the first time photon upconversion employing Si NCs paired with triplet-accepting molecules. Upon excitation, triplet energy transfer occurs over a few tens of nanoseconds by a single Dexter energy transfer step, producing molecular triplet states that can be extracted to fuel upconversion between diffusing molecules in solution. This system upconverts green and red light with 7.0% ± 0.9% efficiency. Losses in this system stem in part from the heterogeneity in the NC synthesis and molecular functionalization, which can be reduced with further improvements in synthetic methodology. When incorporated into aqueous micelles, our upconversion system functions indefinitely under anaerobic conditions and for tens of minutes upon exposure to oxygen. These results stand out among other molecular- and NC-based triplet-fusion upconversion systems, which are typically incompatible with aqueous conditions and exhibit triplet quenching within a few seconds upon exposure to oxygen. Given numerous potential handles for improving our system, we believe that upconversion based on Si NCs can meet the demands of a number of biological applications[3,4,48]. Of even greater importance, our results definitely show that silicon-to-molecule spin-triplet energy transfer is indeed possible, which opens the door to many applications that extend beyond biocompatible upconversion systems. By virtue of its inherent sustainability and environmental compatibility, our silicon-centred approach is highly relevant for quantum information science[25], singlet-fission-driven solar cells[24,49,50] and upconversion photocatalytic systems[1].

Data availability

Experimental data and fits to this data produced using the MATLAB software are available from the authors upon request.

Code availability

The MATLAB code used in the fitting analysis of transient absorption spectra is available from the authors upon request.

Received: 29 May 2019; Accepted: 28 October 2019;

References

1. Ravetz, B. D. et al. Photoredox catalysis using infrared light via triplet fusion upconversion. *Nature* **565**, 343–346 (2019).
2. Tayebjee, M. J. Y., McCamey, D. R. & Schmidt, T. W. Beyond Shockley–Queisser: molecular approaches to high-efficiency photovoltaics. *J. Phys. Chem. Lett.* **6**, 2367–2378 (2015).
3. Chen, S. et al. Near-infrared deep brain stimulation via upconversion nanoparticle–mediated optogenetics. *Science* **359**, 679–684 (2018).
4. Lin, X. et al. Core–shell–shell upconversion nanoparticles with enhanced emission for wireless optogenetic inhibition. *Nano Lett.* **18**, 948–956 (2018).
5. Wu, M. et al. Solid-state infrared-to-visible upconversion sensitized by colloidal nanocrystals. *Nat. Photonics* **10**, 31–34 (2015).
6. Huang, Z. et al. Hybrid molecule–nanocrystal photon upconversion across the visible and near-infrared. *Nano Lett.* **15**, 5552–5557 (2015).
7. Mongin, C., Garakyaraghi, S., Razgoniaeva, N., Zamkov, M. & Castellano, F. N. Direct observation of triplet energy transfer from semiconductor nanocrystals. *Science* **351**, 369–372 (2016).
8. Li, X., Fast, A., Huang, Z., Fishman, D. A. & Tang, M. L. Complementary lock-and-key ligand binding of a triplet transmitter to a nanocrystal photosensitizer. *Angew. Chem. Int. Ed.* **56**, 5598–5602 (2017).
9. Li, X., Huang, Z., Zavala, R. & Tang, M. L. Distance-dependent triplet energy transfer between CdSe nanocrystals and surface bound anthracene. *J. Phys. Chem. Lett.* **7**, 1955–1959 (2016).
10. Garakyaraghi, S. & Castellano, F. N. Nanocrystals for triplet sensitization: molecular behavior from quantum-confined materials. *Inorg. Chem.* **57**, 2351–2359 (2018).
11. Mangolini, L., Thimsen, E. & Kortshagen, U. High-yield plasma synthesis of luminescent silicon nanocrystals. *Nano Lett.* **5**, 655–659 (2005).
12. Limpens, R., Pach, G. F. & Neale, N. R. Nonthermal plasma-synthesized phosphorus–boron co-doped Si nanocrystals: a new approach to nontoxic NIR-emitters. *Chem. Mater.* **31**, 4426–4435 (2019).
13. Hessel, C. M. et al. Synthesis of ligand-stabilized silicon nanocrystals with size-dependent photoluminescence spanning visible to near-infrared wavelengths. *Chem. Mater.* **24**, 393–401 (2012).
14. Wilson, M. W. B. et al. Ultrafast dynamics of exciton fission in polycrystalline pentacene. *J. Am. Chem. Soc.* **133**, 11830–11833 (2011).
15. Burdett, J. J., Müller, A. M., Gosztola, D. & Bardeen, C. J. Excited state dynamics in solid and monomeric tetracene: the roles of superradiance and exciton fission. *J. Chem. Phys.* **133**, 144506 (2010).
16. Sanders, S. N. et al. Quantitative intramolecular singlet fission in bipentacenes. *J. Am. Chem. Soc.* **137**, 8965–8972 (2015).
17. Zirzlmeier, J. et al. Singlet fission in pentacene dimers. *Proc. Natl Acad. Sci. USA* **112**, 5325–5330 (2015).
18. Eaton, S. W. et al. Singlet exciton fission in polycrystalline thin films of a slip-stacked perylenediimide. *J. Am. Chem. Soc.* **135**, 14701–14712 (2013).
19. Le, A. K. et al. Singlet fission involves an interplay between energetic driving force and electronic coupling in perylenediimide films. *J. Am. Chem. Soc.* **140**, 814–826 (2018).
20. Johnson, J. C., Nozik, A. J. & Michl, J. High triplet yield from singlet fission in a thin film of 1,3-diphenylisobenzofuran. *J. Am. Chem. Soc.* **132**, 16302–16303 (2010).
21. Wang, C. & Tauber, M. J. High-yield singlet fission in a zeaxanthin aggregate observed by picosecond resonance Raman spectroscopy. *J. Am. Chem. Soc.* **132**, 13988–13991 (2010).
22. Lukman, S. et al. Efficient singlet fission and triplet-pair emission in a family of zethrene diradicaloids. *J. Am. Chem. Soc.* **139**, 18376–18385 (2017).
23. Hanna, M. C. & Nozik, A. J. Solar conversion efficiency of photovoltaic and photoelectrolysis cells with carrier multiplication absorbers. *J. Appl. Phys.* **100**, 074510 (2006).
24. Futscher, M. H., Rao, A. & Ehrler, B. The potential of singlet fission photon multipliers as an alternative to silicon-based tandem solar cells. *ACS Energy Lett.* **3**, 2587–2592 (2018).
25. Weiss, L. R. et al. Strongly exchange-coupled triplet pairs in an organic semiconductor. *Nat. Phys.* **13**, 176–181 (2017).
26. Einzinger, M. et al. Sensitization of silicon by singlet exciton fission in tetracene. *Nature* **571**, 90–94 (2019).
27. Han, Y. et al. Visible-light-driven sensitization of naphthalene triplets using quantum-confined $CsPbBr_3$ nanocrystals. *J. Phys. Chem. Lett.* **10**, 1457–1463 (2019).
28. Huang, Z. et al. Enhanced near-infrared-to-visible upconversion by synthetic control of PbS nanocrystal triplet photosensitizers. *J. Am. Chem. Soc.* **141**, 9769–9772 (2019).
29. Mahboub, M., Huang, Z. & Tang, M. L. Efficient infrared-to-visible upconversion with subsolar irradiance. *Nano Lett.* **16**, 7169–7175 (2016).
30. Huang, Z. & Tang, M. L. Designing transmitter ligands that mediate energy transfer between semiconductor nanocrystals and molecules. *J. Am. Chem. Soc.* **139**, 9412–9418 (2017).
31. Okumura, K., Mase, K., Yanai, N. & Kimizuka, N. Employing core-shell quantum dots as triplet sensitizers for photon upconversion. *Chem. Eur. J.* **22**, 7721–7726 (2016).
32. Yanai, N. & Kimizuka, N. New triplet sensitization routes for photon upconversion: thermally activated delayed fluorescence molecules, inorganic nanocrystals, and singlet-to-triplet absorption. *Acc. Chem. Res.* **50**, 2487–2495 (2017).
33. Wheeler, L. M. et al. Silyl radical abstraction in the functionalization of plasma-synthesized silicon nanocrystals. *Chem. Mater.* **27**, 6869–6878 (2015).
34. Kroupa, D. M. et al. Control of energy flow dynamics between tetracene ligands and PbS quantum dots by size tuning and ligand coverage. *Nano Lett.* **18**, 865–873 (2018).
35. Bender, J. A. et al. Surface states mediate triplet energy transfer in nanocrystal–acene composite systems. *J. Am. Chem. Soc.* **140**, 7543–7553 (2018).
36. Davis, N. J. L. K. et al. Singlet fission and triplet transfer to PbS quantum dots in TIPS-tetracene carboxylic acid ligands. *J. Phys. Chem. Lett.* **9**, 1454–1460 (2018).
37. Carroll, G. M., Limpens, R. & Neale, N. R. Tuning confinement in colloidal silicon nanocrystals with saturated surface ligands. *Nano Lett.* **18**, 3118–3124 (2018).
38. Montalti, M., Credi, A., Prodi, L. & Gandolfi, M. T. *Handbook of Photochemistry* (CRC Press, Taylor and Francis, 2006).
39. Evans, D. F. Perturbation of singlet–triplet transitions of aromatic molecules by oxygen under pressure. *J. Chem. Soc.* 1351–1357 (1957).
40. Dexter, D. L. A theory of sensitized luminescence in solids. *J. Chem. Phys.* **21**, 836–836 (1953).
41. Yu, Y. et al. Size-dependent photoluminescence efficiency of silicon nanocrystal quantum dots. *J. Phys. Chem. C* **121**, 23240–23248 (2017).
42. Stolle, C. J., Lu, X., Yu, Y., Schaller, R. D. & Korgel, B. A. Efficient carrier multiplication in colloidal silicon nanorods. *Nano Lett.* **17**, 5580–5586 (2017).
43. Garakyaraghi, S., Mongin, C., Granger, D. B., Anthony, J. E. & Castellano, F. N. Delayed molecular triplet generation from energized lead sulfide quantum dots. *J. Phys. Chem. Lett.* **8**, 1458–1463 (2017).
44. Sanders, S. N., Gangishetty, M. K., Sfeir, M. Y. & Congreve, D. N. Photon upconversion in aqueous nanodroplets. *J. Am. Chem. Soc.* **141**, 9180–9184 (2019).
45. Kouno, H., Sasaki, Y., Yanai, N. & Kimizuka, N. Supramolecular crowding can avoid oxygen quenching of photon upconversion in water. *Chem. Eur. J.* **25**, 6124–6130 (2019).
46. Kim, J.-H. & Kim, J.-H. Encapsulated triplet–triplet annihilation-based upconversion in the aqueous phase for sub-band-gap semiconductor photocatalysis. *J. Am. Chem. Soc.* **134**, 17478–17481 (2012).
47. Marsico, F. et al. Hyperbranched unsaturated polyphosphates as a protective matrix for long-term photon upconversion in air. *J. Am. Chem. Soc.* **136**, 11057–11064 (2014).
48. Weissleder, R. A clearer vision for in vivo imaging. *Nat. Biotechnol.* **19**, 316–317 (2001).
49. Dexter, D. L. Two ideas on energy transfer phenomena: ion-pair effects involving the OH stretching mode, and sensitization of photovoltaic cells. *J. Lumin.* **18**, 779–784 (1979).
50. MacQueen, R. W. et al. Crystalline silicon solar cells with tetracene interlayers: the path to silicon-singlet fission heterojunction devices. *Mater. Horiz.* **5**, 1065–1075 (2018).

Acknowledgements

S.T.R. and E.K.R. acknowledge support from the National Science Foundation (CHE-1610412), the Robert A. Welch Foundation (Grant F-1885) and the Research Corporation for Science Advancement (Grant #24489). E.K.R. would also like to acknowledge partial support from a Leon O. Morgan fellowship. M.L.T. acknowledges an Air Force Office of Scientific Research (AFOSR) Award (FA9550-19-1-0092) for equipment and the DOE (DE-SC0018969) for salary support. L.M. and D.C. acknowledge support from the National Science Foundation under CAREER award #1351386.

Author contribution

Hydrogen-terminated Si NC were synthesized by D.C. P.X. and C.S.G. functionalized the Si NCs with organic ligands, characterized their steady-state properties and performed upconversion measurements. E.K.R. conducted transient absorption experiments and analysed the resulting data. L.M., M.L.T. and S.T.R. oversaw the project. P.X., E.K.R., L.M., M.L.T. and S.T.R. composed the manuscript.

Competing interests

The authors declare no competing interests.

Additional information

Supplementary information is available for this paper at https://doi.org/10.1038/s41557-019-0385-8.

Correspondence and requests for materials should be addressed to L.M., M.L.T. or S.T.R.

QUERY FORM

Nature Chemistry	
Manuscript ID	**[Art. Id: 385]**
Author	**Pan Xia**

AUTHOR:

The following queries have arisen during the editing of your manuscript. Please answer by making the requisite corrections directly in the e.proofing tool rather than marking them up on the PDF. This will ensure that your corrections are incorporated accurately and that your paper is published as quickly as possible.

Query No.	*Nature of Query*
Q1:	Please provide a suitable graphic for the contents list.
Q2:	Please check your article carefully, coordinate with any co-authors and enter all final edits clearly in the eproof, remembering to save frequently. Once corrections are submitted, we cannot routinely make further changes to the article.
Q3:	Note that the eproof should be amended in only one browser window at any one time; otherwise changes will be overwritten.
Q4:	Author surnames have been highlighted. Please check these carefully and adjust if the first name or surname is marked up incorrectly. Note that changes here will affect indexing of your article in public repositories such as PubMed. Also, carefully check the spelling and numbering of all author names and affiliations, and the corresponding email address(es).
Q5:	You cannot alter accepted Supplementary Information files except for critical changes to scientific content. If you do resupply any files, please also provide a brief (but complete) list of changes.
Q6:	In the e.proof tool, the numbers for those compounds that will be deposited in PubChem do not appear bold, and the link is not visible. You do not need to amend this, they will appear correctly once published online.
Q7:	In the sentence beginning 'Moreover,' is the change to 'spin-triplet' correct?
Q8:	In the sentence beginning 'Due to its dominance', and elsewhere in the Introduction, should 'junction(s)' be changed to 'heterojunction(s)'?
Q9:	In the sentence beginning 'This yields', inset has been removed from the citation to Fig. 1b because the structures of the modified Si NCs are shown in the main figure and not in the inset.
Q10:	In the bottom part of Fig. 1a, should there be an arrow from the unlabelled bar (second from the right) to the bar labelled S*?
Q11:	In the caption to the inset of Fig. 3b, please check the changes to the text are correct and that the key to the spectra is correct.
Q12:	For completeness, should the sentence beginning 'Upon hydrosilylation with 9VA' be changed to 'Upon hydrosilylation with 1-octadecene and 9VA'?
Q13:	In the sentence beginning 'Nuclear magnetic', would 9VA be better changed to 9EA as this is the species actually bound to the NC?

QUERY FORM

Nature Chemistry	
Manuscript ID	**[Art. Id: 385]**
Author	**Pan Xia**

AUTHOR:

The following queries have arisen during the editing of your manuscript. Please answer by making the requisite corrections directly in the e.proofing tool rather than marking them up on the PDF. This will ensure that your corrections are incorporated accurately and that your paper is published as quickly as possible.

Query No.	*Nature of Query*
Q14:	In the sentence beginning 'DPA was chosen', T1 has been replaced by E (two instances) as the former is a symbol for triplet whereas E represents energy, which is what the number represents. Is this ok?
Q15:	Please check changes to the caption to Fig. 2a are correct.
Q16:	In Fig. 2a, please indicate either in the figure or in the caption what the arrow refers to.
Q17:	No inset has been provided for Fig. 2a. Would you like to delete this line or provide an inset?
Q18:	In Fig. 2b,c, λexc and Nexc have been changed to λEx and NEx for consistency throughout the paper. Ok?
Q19:	In the caption to Fig. 2b, please provide and explanation for the axis labelling at the top of the figure.
Q20:	Is the definition of CW correct in the caption to Fig. 2c?
Q21:	In Fig. 2c, do the symbols < > represent average? If not, please indicate what they mean.
Q22:	'(left)' has been inserted after Figure 3a in the sentence beginning with 'Figure 3a'. Ok?
Q23:	In the y axis label in Fig. 3c, is (mOD) correct? In this case what does the m represent?
Q24:	Should the start of the sentence beginning 'Isolating this new feature' be changed to 'Isolating these new features'? If not, which feature do you refer to?
Q25:	In the sentence beginning 'The impact', it states that the Si signal persists after the decay of 9EA, referring to Fig. 3c. However, this persistence beyond 9EA is not shown in Fig. 3c, is this ok?
Q26:	In the sentence beginning 'Decay parameters', rate has been changed to rate constant when referring to the parameters k. Ok?
Q27:	In the sentence beginning 'Overall' and also in the caption to Fig. 4b, will the term 'decades' be widely understood or would this be better changed to 'over time spanning a few nanoseconds to tens of microseconds'?
Q28:	In the Arrhenius relation in Fig. 4a, should the * sign be changed to a '~' (proportional to) sign?
Q29:	In the captions to Fig. 4b,c, please indicate which lines are observed data and which are fits.
Q30:	In the sentence beginning 'Of the remaining' is 'excitations' correct or should it be changed to 'excitons'?
Q31:	In the sentence beginning 'Using methods', poly(propylene oxide) has been inserted to indicate the nature of the phydrophobic core. Is this correct?

QUERY FORM

Nature Chemistry	
Manuscript ID	**[Art. Id: 385]**
Author	**Pan Xia**

AUTHOR:

The following queries have arisen during the editing of your manuscript. Please answer by making the requisite corrections directly in the e.proofing tool rather than marking them up on the PDF. This will ensure that your corrections are incorporated accurately and that your paper is published as quickly as possible.

Query No.	*Nature of Query*
Q32:	In the sentence beginning 'P188', is the definition of USFDA correct?
Q33:	In the sentence beginning 'Within the core', is the definition of ODCB correct?
Q34:	In Fig.5c, should '(arb. units)' be placed after PL in the y axis label?
Q35:	In the sentence beginning 'Upon illumination', is 512 nm correct or should it be changed to 532 nm, as used in other experiments?
Q36:	Please check that the change to the journal title in ref. 17 is correct.
Q37:	In ref. 23, is the change to the article number correct?
Q38:	In ref. 40, please give page range or is there only one page?